



Alexandria University
Alexandria Engineering Journal

www.elsevier.com/locate/aej
www.sciencedirect.com



ORIGINAL ARTICLE

Strengthening of RC bridge slabs using CFRP sheets



Fahmy A. Fathelbab, Mostafa S. Ramadan, Ayman Al-Tantawy *

Structural Engineering Department, Faculty of Engineering, Alexandria University, Egypt

Received 7 October 2013; revised 30 August 2014; accepted 16 September 2014

Available online 18 October 2014

KEYWORDS

Slab;
Strengthening;
CFRP;
FEM;
ANSYS;
Modeling

Abstract Many old structures became structurally insufficient to carry the new loading conditions requirements. Moreover, they suffer from structural degradation, reinforcement steel bars corrosion, bad weather conditions...etc. Many official authorities in several countries had recognized many old bridges and buildings as structurally deficient by today's standards. Due to these reasons, structural strengthening became an essential requirement and different strengthening techniques appeared in market. Fiber Reinforced Polymer (FRP) strengthening techniques established a good position among all other techniques, giving excellent structural results, low time required and moderate cost compared with the other techniques. The main purpose of this research is to study analytically the strengthening of a reinforced concrete bridge slabs due to excessive loads, using externally bonded FRP sheets technique. A commercial finite element program ANSYS was used to perform a structural linear and non-linear analysis for strengthened slab models using several schemes of FRP sheets. A parametric study was performed to evaluate analytically the effect of changing both FRP stiffness and FRP schemes in strengthening RC slabs. Comparing the results with control slab (reinforced concrete slab without strengthening) it is obvious that attaching FRP sheets to the RC slab increases its capacity and enhances the ductility/toughness.

© 2014 Production and hosting by Elsevier B.V. on behalf of Faculty of Engineering, Alexandria University.

1. Introduction

Strengthening of structural members using Fiber-Reinforced Polymer (FRP) is one of the most powerful methods to enhance and raise the capacity of an individual members as well as the whole structure to resist the applied loads in its different levels, which are greater than the resistance capacity of

the structure without strengthening. Strengthening improves the mechanical properties of an individual member along with the whole structure up to failure like ductility, toughness, cracking behavior and post-buckling behavior [1,6].

The benefits of strengthening with FRP became obvious when a large number of reinforced concrete bridges in USA and other countries are structurally deficient by today's standards [7]. The main contributing factors lead to the need of the strengthening were change in structure use, increase in load requirements, corrosion deterioration due to exposure to an aggressive environment, or the desire to enhance the structure behavior under certain load type like cyclic loads. In order to

* Corresponding author. Tel.: +20 1003368911, +965 60072918.

E-mail address: asatstr@yahoo.com (A. Al-Tantawy).

Peer review under responsibility of Faculty of Engineering, Alexandria University.

preserve those bridges, rehabilitation considered essential to maintain their capability and to increase public safety Kachlakev et al. [5].

Many researchers have found that FRP composite strengthening is an efficient, reliable, and cost-effective means of rehabilitation [5]. American Concrete Institute committee 440 (ACI 440) established design recommendations and guidelines for FRP applications to reinforced concrete whether strengthening or design.

FRP typically organized in a laminate structure, such that each lamina (or flat layer) contains an arrangement of unidirectional fibers or woven fiber fabrics embedded within a thin layer of light polymer matrix material. Fibers are typically composed of carbon, aramid or glass, provide the strength and stiffness. The matrix is commonly made of polyester, epoxy, or nylon, binds to protect the fibers from damage, and to transfer the stresses between fibers. There are two additional types of FRP composite, bidirectional fibers which are used commonly for strengthening and design the two-way slab, and the FRP robs which became competitor alternative for reinforcement steel bars [8].

2. Literature review

Vasquez and Karbhari [9] studied experimentally six real scale specimens; the authors studied the failure mechanisms and post-debonding response. The first and the fourth specimens were rectangular slabs 6.0 m length, 3.20 m width and 0.18 m thickness with reinforcement mesh top and bottom, the rest of specimens were with cutout as rectangular opening measuring 1.0 m length and 1.60 m width cut in the center of each slab specimen. The specimens were divided into two groups based on the configuration of the loading. Group “A” consists of the first 3 specimens loaded in two points, spacing between them 2.36 m at mid line of the slabs length. Group “B” consists of the next 3 specimens loaded in two points spacing between them 2.30 m at mid line of the slabs width. The authors stated that, for group “A” after removal of the cutout region in the un-strengthened slab the first yield noticed at load 4.5 ton, the slab suffer of increasing flexure cracks in length and deflection beyond the first crack till failure which took place at load 6.7 ton. In case of the strengthened slab, failure was due to debonding of FRP strips, in load of first yield only very short and thin hairline cracks noted, the first indication of damage was noticed through cracking of adhesive at a load of 5.8 ton. The strip closest to the edge of the cutout showed the first signs of local debonding with cracking of cover concrete at a load of 16.3 ton, subsequent to which the load increased with progressive increase in peeling of the strips within the concrete cover up to a load of 16.7 ton.

Arduini et al. [2] studied experimentally 26 real scale slabs; the strengthening system consisted of CFRP laminates applied by manual lay-up, Type S with no overhang, and Type C with a cantilevered overhang. Each group was further divided into four sets (T1–T4) based on different amounts of internal steel reinforcement in tension and compression. Within each slab set, two different levels of CFRP strengthening (L1–L2) were investigated. The typical slab was 5.0 m length, 1.5 m width, and 0.24 m thickness with mesh reinforcement top and bottom. The bending tests that were carried out in the laboratory by a hydraulic jack provided the load that operated under displacement control. The authors stated that, the FRP ultimate strain for specimen (S-T2L2) that failed by concrete shear is very low while the strain in (S-T2L1) that failed by fiber rupture is approximately 0.0082. Specimens (S-T2L2) and (S-T4L2) showed extensive flexural cracking prior to failure, for specimens (S-T1L2), (S-T3L2), and (S-T4L1) the failure was by FRP laminate peeling starting at a flexural crack and progressing towards the support, and pre-cracking of the slab prior to FRP installation did not greatly influence the overall flexural performance of the member.

Ebead and Marzouk [3] studied experimentally 9 two way square slabs 1.90 m dimensions and 0.15 m thickness with different reinforcement amounts, the test specimens were simply supported along the four edges with corners free to lift and were centrally loaded through the column stub. The authors determined the reinforcement ratio depending on the failure mode, whereas the failure mode of slabs with reinforcement ratios less than or equal to 0.5% is normally a flexural mode and for reinforcement ratios of 1.0% or more are likely to fail due to a punching shear mode. The authors stated that, specimens with a reinforcement ratio of 0.35% indicated the lowest first crack loads of 7.3, 7.0, and 6.8 ton, the first crack loads of 8.4, 8.0, and 8.3 ton recorded for the specimens with reinforcement ratio of 0.5%, the first crack loads were 8.9, 10.3, and 9.6 ton for specimens with reinforcement ratio of 1.0%. The use of CFRP (Carbon Fiber Reinforced Polymer) and GFRP (Glass Fiber Reinforced Polymer) increased the equivalent reinforcement ratio slightly compared with the reference specimens. The deflection value decreased as the reinforcement ratio increased, the deflection at the ultimate load decreased from 42 to 24 mm as the reinforcement ratio increased from 0.35% to 1.0%. For the flexural strengthening specimens, the slope of the load–deflection curve was higher than that of the corresponding reference specimens, the average deflection at the ultimate load of the flexural strengthening specimens was approximately 0.6 that of the corresponding reference specimens. The flexural strengthening specimens experienced a smaller deformation compared to the corresponding refer-

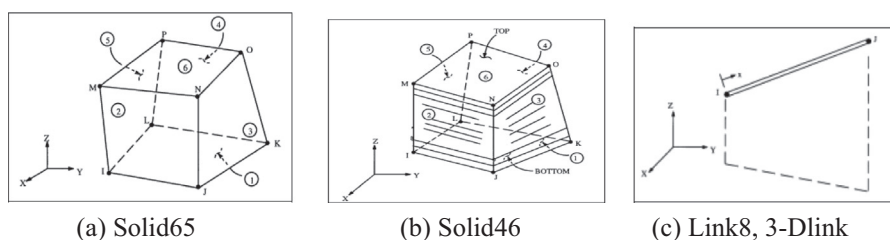


Figure 1 Used modeling elements.

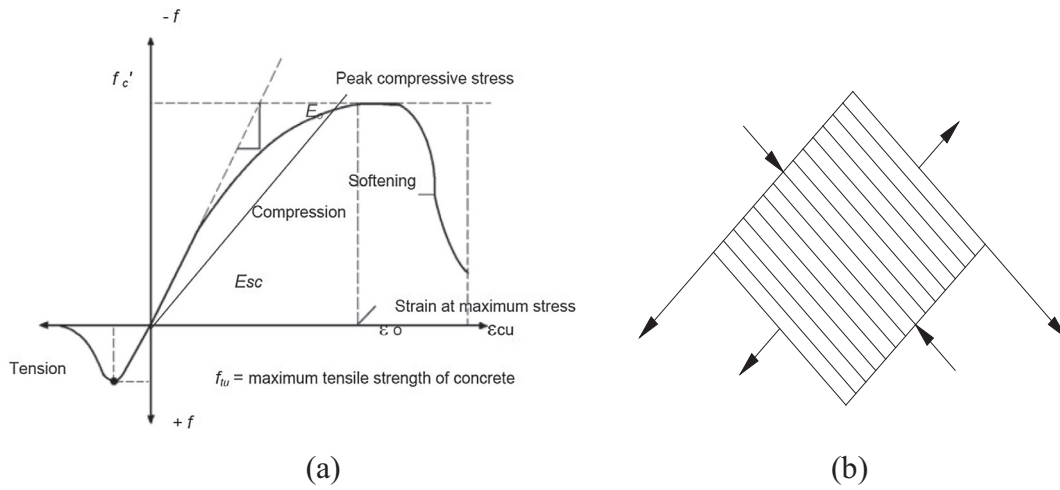
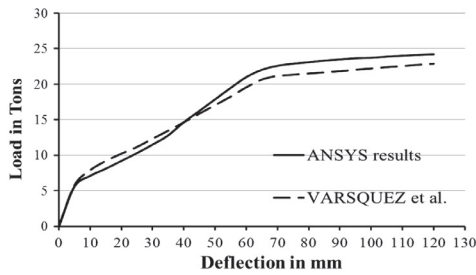
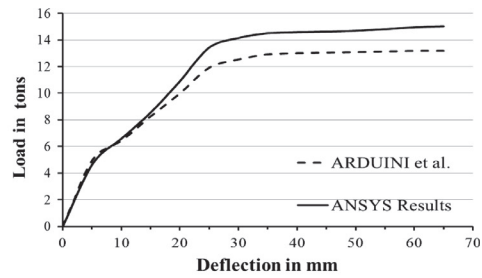


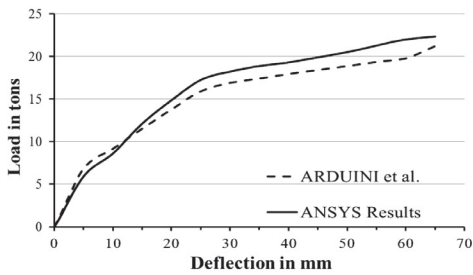
Figure 2 (a) Stress-strain curve, and (b) smeared crack.



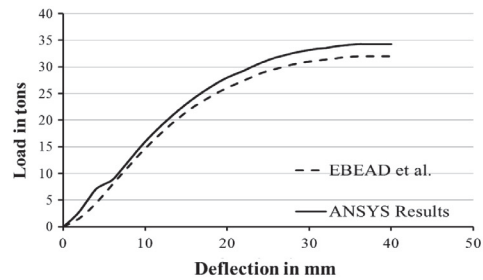
(1) First verification level



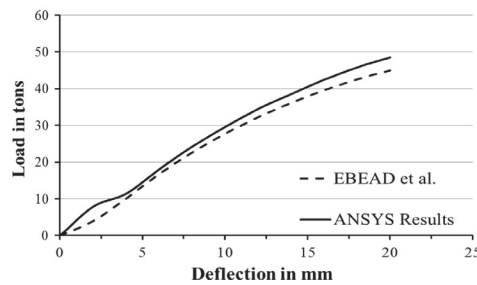
(2) Second verification level



(3) Third verification level



(4) Fourth verification level



(5) Fifth verification level

Figure 3 Comparison curves for different verification levels.

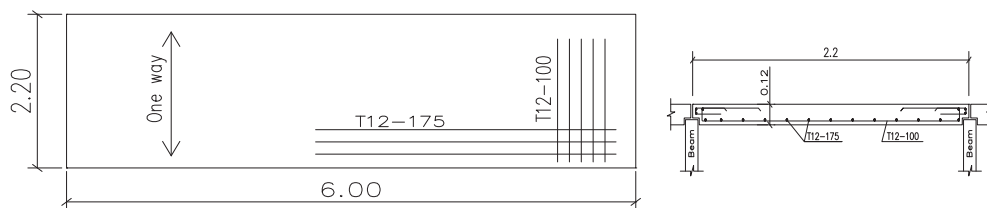


Figure 4 Plan and cross section details of the slab model, dimensions in meter.

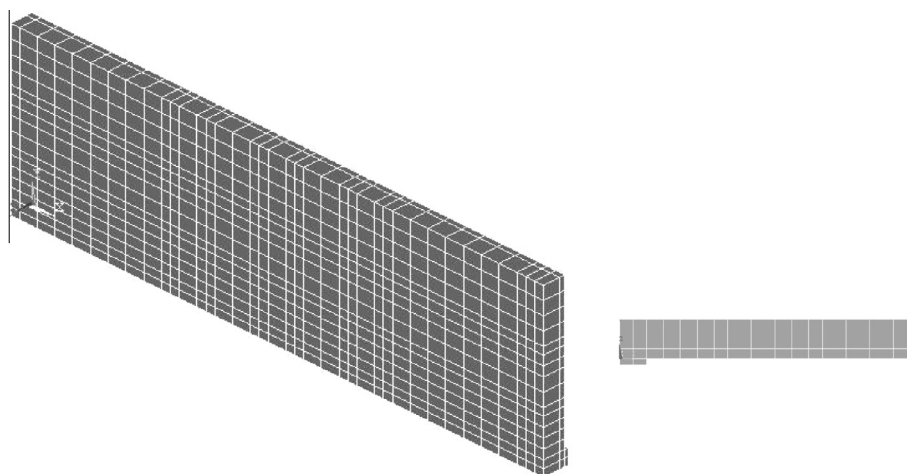


Figure 5 3D and elevation of ANSYS model.

Table 1 CFRP flexure schemes attached to slab soffit.

Model ID	FN	Attachment configuration
S-0	–	Control slab – without strengthening
S-1	1	FW = 100 mm, FL = 1S = 2.1 m, and FS = 1.0 m
S-2	1	FW = 100 mm, FL = 1S = 2.1 m, and FS = 0.6 m
S-3	1	FW = 100 mm, FL = 1S = 2.1 m, and FS = 0.3 m
S-4	2	FW = 100 mm, FL = 1S = 2.1 m, and FS = 0.3 m
S-5	3	FW = 100 mm, FL = 1S = 2.1 m, and FS = 0.3 m
S-6	3	FW = 100 mm, FL = 2/3S = 1.40 m, and FS = 0.3 m
S-7	3	FW = 100 mm, FL = 1/3S = 0.80 m, and FS = 0.3 m
S-8	1	FW = 200 mm, FL = 1S = 2.1 m, and FS = 1.5 m
S-9	1	FW = 200 mm, FL = 1S = 2.1 m, and FS = 1.0 m
S-10	1	FW = 200 mm, FL = 1S = 2.1 m, and FS = 0.5 m
S-11	2	FW = 200 mm, FL = 1S = 2.1 m, and FS = 0.5 m
S-12	3	FW = 200 mm, FL = 1S = 2.1 m, and FS = 0.5 m
S-13	3	FW = 200 mm, FL = 2/3S = 1.40 m, and FS = 0.5 m
S-14	3	FW = 200 mm, FL = 1/3S = 0.80 m, and FS = 0.5 m
S-15	2	FW = full slab length, and FL = 2/3S = 1.4 m
S-16	3	FW = full slab length, and FL = 2/3S = 1.4 m

ence specimens due to the effect of the FRP materials on the overall behavior of the slabs, regarding the punching-shear-strengthening.

3. Finite element modeling

ANSYS computer program used in the analysis of different mechanical and structural applications based on the finite element modeling techniques. SOLID65 element is used to model the plain concrete material, since it has a capability of both

cracking in tension and crushing in compression, SOLID65 element is defined by 8 nodes with three degrees of freedom at each node; translations in the nodal x, y, and z directions. The element material was assumed initially isotropic. The most important aspect of this element is the treatment of nonlinear material properties, where concrete is capable of directional cracking and crushing besides incorporating plastic and creep behavior. The LINK8 element was used to model the reinforcing steel bar; it is uniaxial tension-compression member, which can include nonlinear material properties. The element

comprises two nodes with three degree of freedom at each one, the elastic-perfectly plastic representation was assumed for the reinforcing steel bars. The SOLID46 layered structural solid element was used to model the CFRP materials, the element comprises 8 nodes with three degrees of freedom at each node. The element material is assumed to be orthotropic and no slippage is assumed between the element layers (perfect interlaminar bond). Whereas, CFRP sheets are brittle materials, the

stress-strain relationship is roughly linear up to failure. Consequently, in this study, it is assumed that the stress-strain relationships for the CFRP laminates are linearly elastic; the elements are shown in Fig. 1.

The suggested stress-strain relationship for the concrete represents both the ascending and descending portions. This relation provides two parameters, one to adjust the ascending portion and the other to control the descending portion.

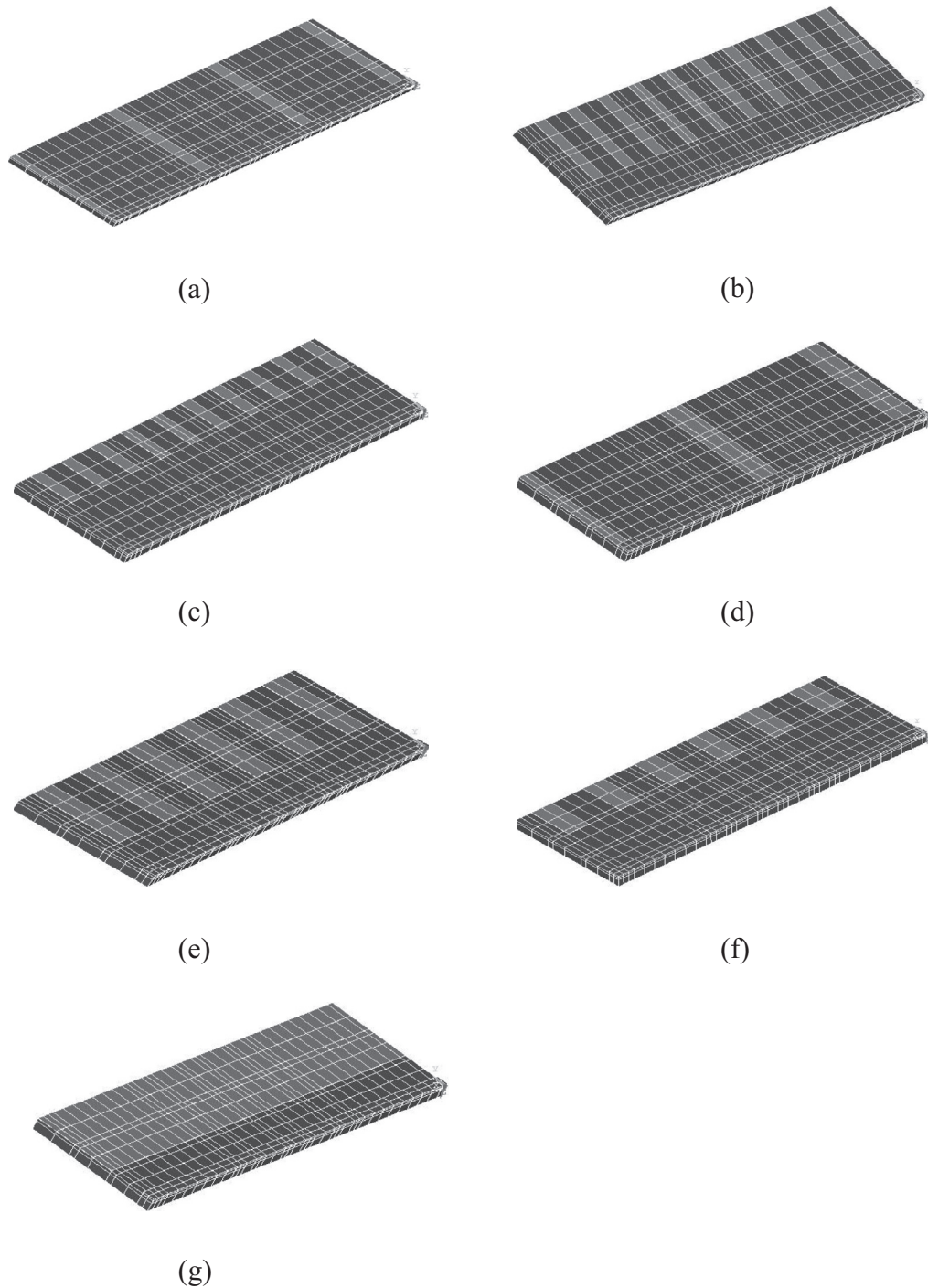


Figure 6 Soffit view of strengthened slabs, (a) ANSYS models S-1 to S-5, (b) ANSYS model S-6, (c) ANSYS model S-7, (d) ANSYS models S-8 to S-12, (e) ANSYS model S-13, (f) ANSYS model S-14, and (g) ANSYS models S-15 and S-16.

Because of its simplicity and experimental validation, the stress–strain relation suggested by Ghoniem [4] is utilized in the present study, as shown in Fig. 2. This relation is given as:

$$Y = \frac{mX}{1 + \left[m - \frac{n}{(n-1)} \right]^2 X + \frac{X^n}{(n-1)}}$$

where

$Y = f/f'_c$ the ratio of the concrete stress to the ultimate concrete strength,

$X = \varepsilon/\varepsilon_0$ the ratio of the concrete strain to the strain at $Y = 1$,

$m = E_0/E_{sc}$ the ratio of the initial tangent modulus to the secant modulus at $Y = 1$,

n a factor to control the slope and curvature of the descending portion,

the parameters (m, n) are given below and are based on test data,

$m = 1 + (17.9/f'_c)$, f'_c in N/mm^2 , $n = (f'_c/6.68) - 1.85 > 1.0$,

in this case, the secant modulus is given as $E_{sc} = E_0/m$.

Cracking and crushing are the most significant factors contributing to nonlinear behavior of concrete. The crack modeling adopted by ANSYS program is the smeared crack representation. Where shear transfer coefficient (βt) represents the reduction factor of shear strength for the subsequent loads, which induces sliding (shear) across the crack face. If the crack closes, then all compressive stresses normal to the crack plane transmitted and only a shear reduction factor (βc) for a closed crack introduced. Typical shear transfer coefficients range from zero, which represents a smooth crack to one, which represents a rough crack. In the present analysis $\beta t = 0.1$ and $\beta c = 0.8$.

The concrete model material predicts the failure of brittle materials. Both cracking and crushing failure modes are accounted for. The failure criterion of concrete due to a multi-axial stress state is expressed in the form:

$$\frac{f}{f_{cu}} - S > 0.0$$

where

f function of the principal stress state (f_{xp}, f_{yp}, f_{zp}) in the principal directions,

S failure surface expressed in terms of principal stresses,

f_{cu} uniaxial crushing strength.

The material will crack if any principal stress is tensile with a crack plane normal to this principal stress, while crushing will take place only if all principal stresses are compressive.

4. Computer modeling verification

Verification of ANSYS models passes through five verification levels. The first three levels are one-way slab, the first and second are one way slabs with different reinforcement combinations and were analyzed nonlinearly, Vasquez et al. [9] and Arduini et al. [2]; the third one is one way slab strengthened in flexure using CFRP, Arduini et al. [2]. The fourth and fifth are two way slabs loaded by short column in mid span and was designed to fail at flexure by limiting the reinforcement ratio not to exceed than 1% (Ebead and Marzouk [3]), the fourth

one strengthened in flexure using CFRP sheets. All the five verification models were analyzed nonlinearly.

Fig. 3 shows the verification results in form of comparison curves for each verification level.

Modeling of structural reinforced concrete elements using FE program (ANSYS) proves the ability of modeling and analyzing the reinforced concrete elements in all circumstances including strengthening cases. Since the above verification levels results had shown a good agreement between FE modeling procedures using ANSYS and the results from published papers. Therefore, the coming parametric study will get intensity, reliability, and credibility.

5. The parametric study

The model used in this study is a real scale one-way slab in a bridge (built in USA, Oregon State, 1938) with dimensions of 2.2×6.0 m and 12 cm thickness, refer to Fig. 4 for cross section details and reinforcement. Material properties briefed below:

Concrete

$f_{cu} = 25 \text{ N/mm}^2$, $f_t = 2.0 \text{ N/mm}^2$ $E_c = 19,000 \text{ N/mm}^2$
Poisson's ratio = 0.2

Stress–strain curve was according to Ghoniem [4].

Reinforcement Steel

Steel grade 36/52, $f_y = 360 \text{ N/mm}^2$, $E_s = 200,000 \text{ N/mm}^2$
Poisson's ratio = 0.3

CFRP (Carbon Fiber Reinforced Polymer) sheets

Layer thickness = 1.0 mm, Tensile strength $f_u = 958 \text{ N/mm}^2$

$E_x = 62,000 \text{ N/mm}^2$, $E_y = 4800 \text{ N/mm}^2$ and $E_z = 4800 \text{ N/mm}^2$

Poisson's ratios:

$v_{xy} = 0.22$ $v_{xz} = 0.22$ $v_{yz} = 0.3$

$G_{xy} = 3270 \text{ N/mm}^2$ $G_{xz} = 3270 \text{ N/mm}^2$ $G_{yz} = 1860 \text{ N/mm}^2$

5.1. Finite element model

One quarter of the slab was modeled using ANSYS software; Fig. 5 shows the model.

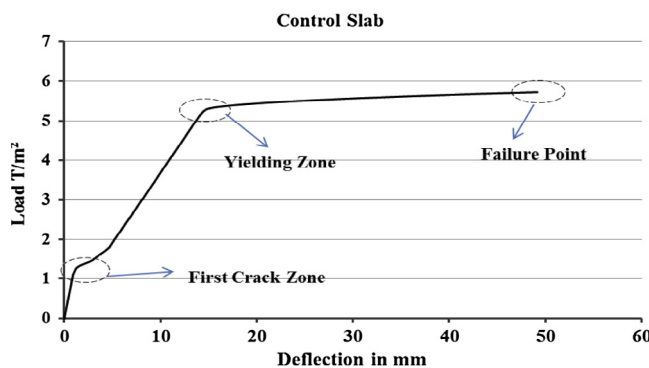


Figure 7 Load–deflection curve for control slab.

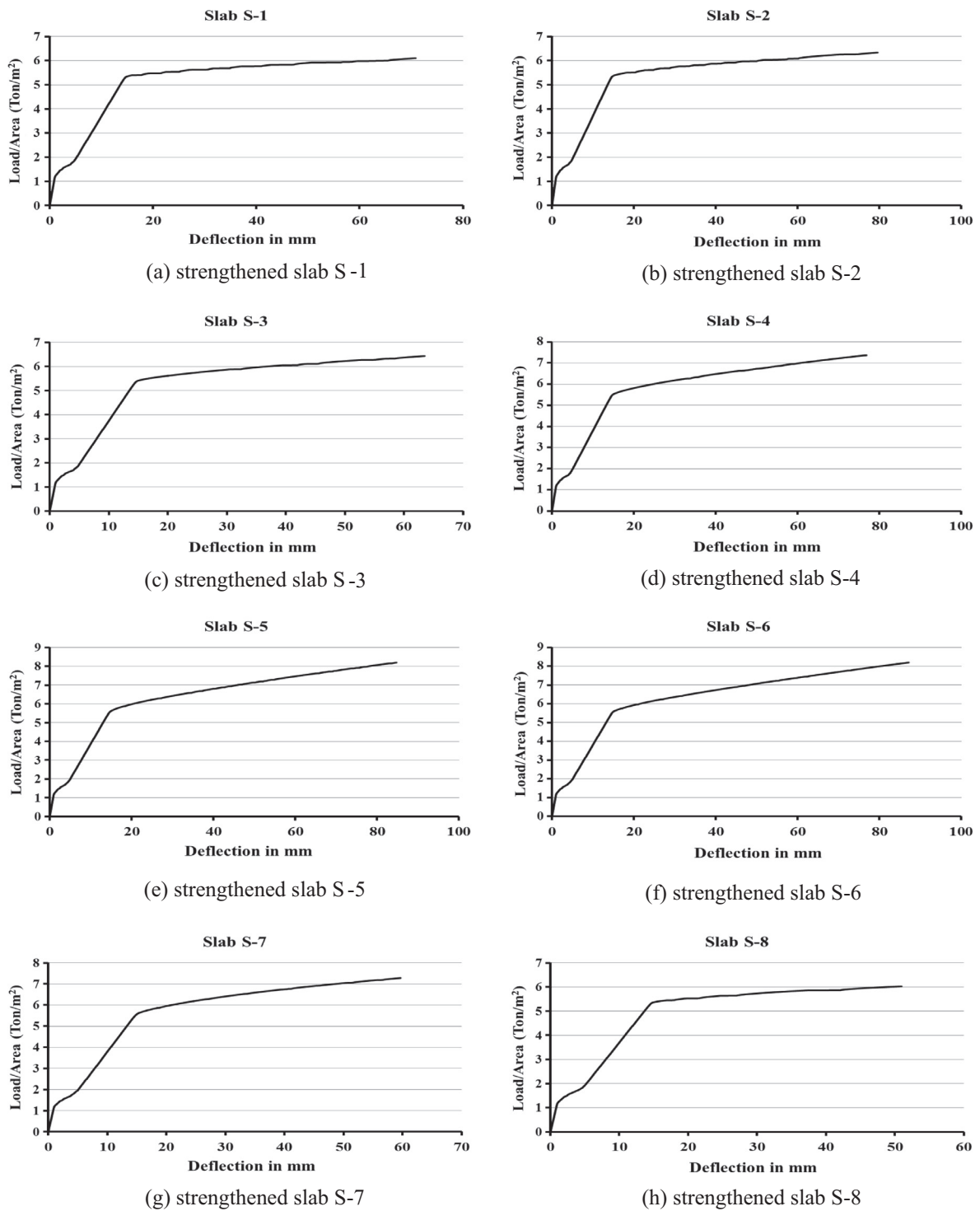


Figure 8 (a) Strengthened slab S-1, (b) strengthened slab S-2, (c) strengthened slab S-3, (d) strengthened slab S-4, (e) strengthened slab S-5, (f) strengthened slab S-6, (g) strengthened slab S-7, (h) strengthened slab S-8, (i) strengthened slab S-9, (j) strengthened slab S-10, (k) strengthened slab S-11, (l) strengthened slab S-12, (m) strengthened slab S-13, (n) strengthened slab S-14, (o) strengthened slab S-15, and (p) strengthened slab S-16.

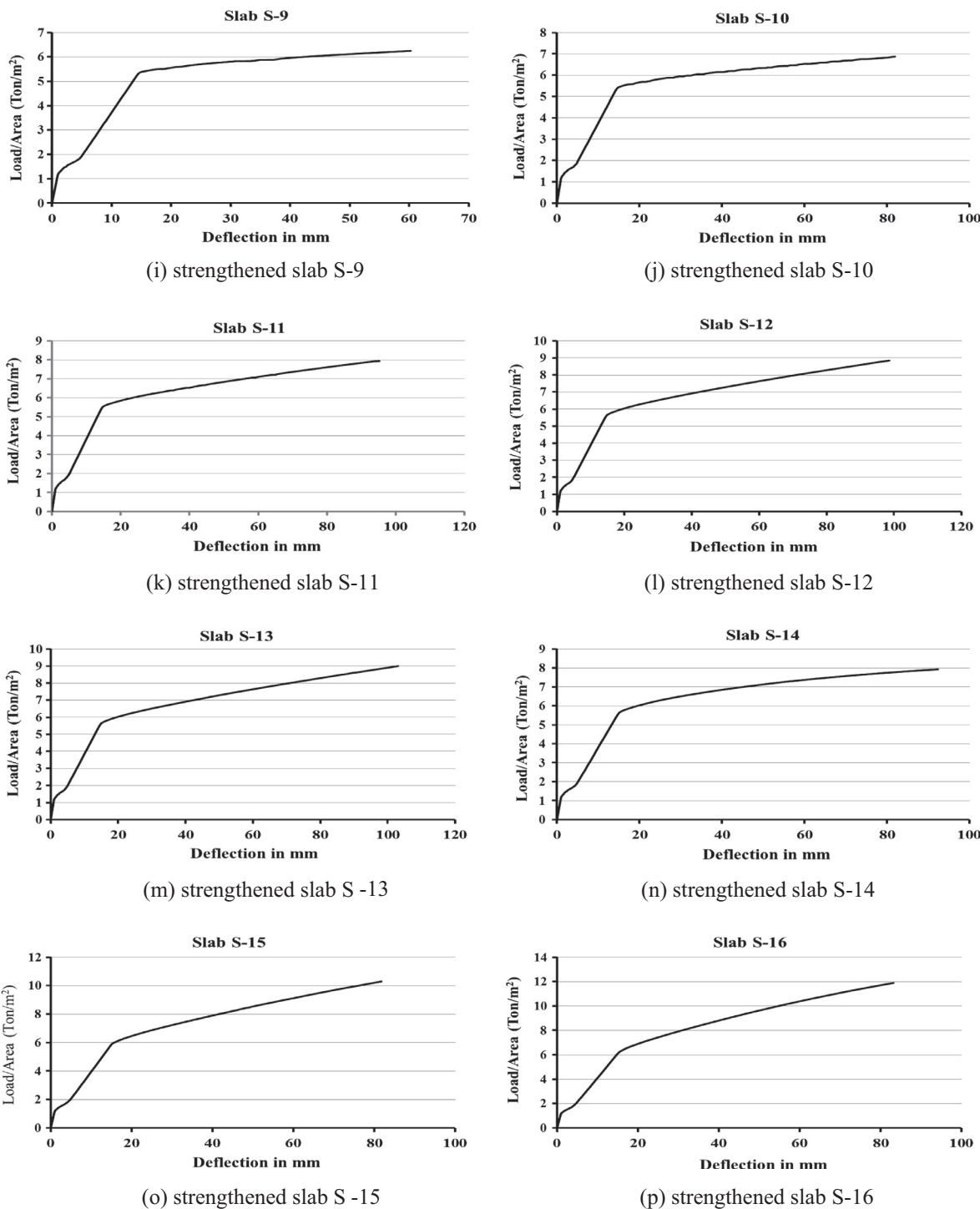


Fig 8. (continued)

5.2. Variables of the study

The study deals with four variables as follows:

1. The first one is CFRP sheet width, $FW = 100$ mm, 200 mm, and full length of slab.
2. The second one is CFRP sheet length, FL taken as function of slab short span “S”, $FL = 1S, 2/3S, 1/3S$.

3. The third one is CFRP sheet spacing, $FS = 1.5$ m, 1.0 m, 0.6 m, 0.5 m, and 0.3 m.
4. The fourth one is number of CFRP plies = $1, 2,$ and 3 .

The CFRP ply thickness is constant for all cases and equals to 1.0 mm. Table 1 summarizes different studied CFRP schemes attached to slab soffit, the number of plies, thickness of each ply, and configuration of plies. Fig. 6 shows ANSYS different models according to attachment configuration.

Table 2 Loads' values at different stages of loading.

Model ID	First cracking load (T/m ²)	Yielding load (T/m ²)	Ultimate load (T/m ²)	Increase in ultimate load compared to control slab (%)
Control slab	1.04	5.25	5.73	N/A
S.1	1.04	5.29	6.10	6.58
S.2	1.05	5.33	6.34	10.66
S.3	1.04	5.38	6.43	12.32
S.4	1.04	5.50	7.37	28.68
S.5	1.04	5.57	8.20	43.21
S.6	1.04	5.57	8.20	43.21
S.7	1.05	5.58	7.28	27.17
S.8	1.05	5.34	6.03	5.26
S.9	1.05	5.36	6.25	9.17
S.10	1.04	5.42	6.88	20.09
S.11	1.05	5.53	7.93	38.50
S.12	1.06	5.66	8.85	54.51
S.13	1.05	5.64	8.85	54.51
S.14	1.05	5.66	7.93	38.47
S.15	1.07	5.96	10.30	79.81
S.16	1.08	6.27	11.90	107.74

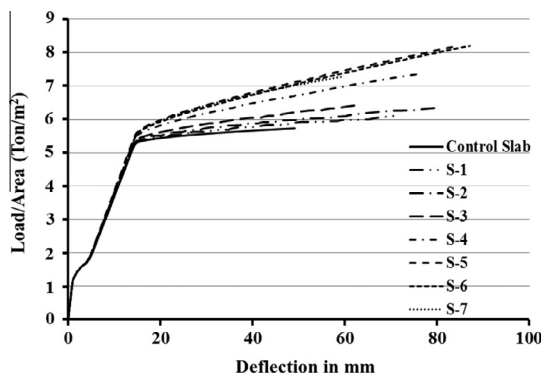


Figure 9 Grouped load–deflection curves S-1 to S-7.

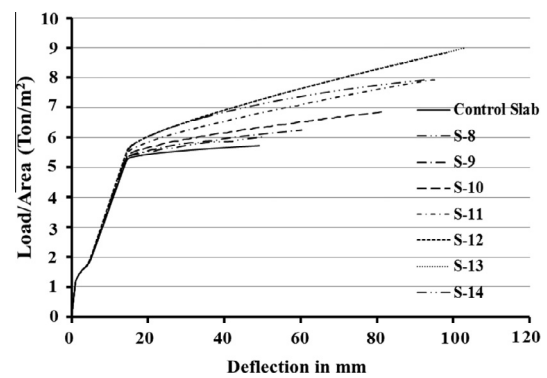


Figure 11 Grouped load–deflection curves S-8 to S-14.

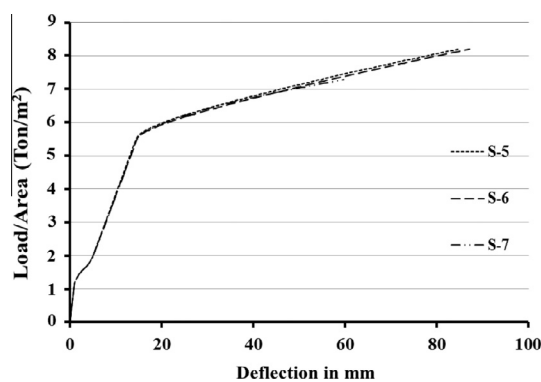


Figure 10 Grouped load–deflection curves S-5 to S-7.

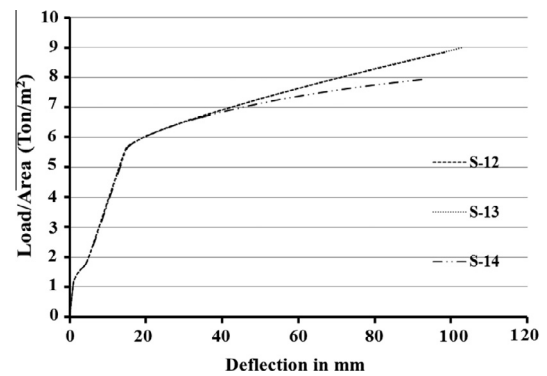


Figure 12 Grouped load–deflection curves S-12 to S-14.

5.3. Summary of ANSYS results

5.3.1. Control slab results (S-0)

Fig. 7 shows the load–deflection curve for the control slab. The figure indicates that the first crack occurs at load equals to 1.43 Ton/m², yielding occurs at 5.25 Ton/m² and the ultimate occurs at 5.726 Ton/m².

5.3.2. Strengthened slabs results (S-1 to S-16)

Sixteen strengthened slab in flexure using CFRP sheets in different schemes, as shown in Table 1 are analyzed and studied analytically using finite element program ANSYS.

Fig. 8 (a : p) shows the load–deflection curves for flexure-strengthened slabs models S-1 to S-16.

Table 2 summarizes the result values of first crack load, yielding load and ultimate load for each strengthened slab model.

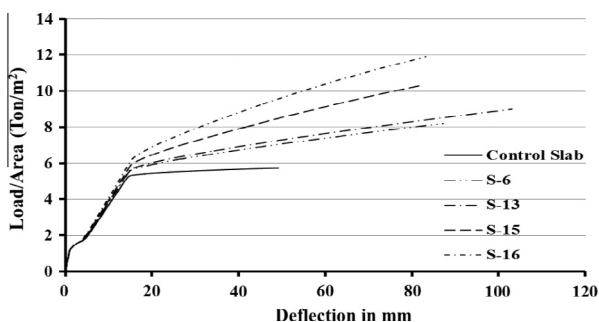


Figure 13 Grouped load-deflection curves S-6, S-13, S-15, and S-16.

5.4. Comparison and discussion of the results

5.4.1. Load versus deflection curves

Fig. 9 shows grouped load-deflection curves for flexural strengthened slabs S-1 to S-7, it is obvious that by increasing

the number of CFRP plies and decreasing the spacing between CFRP sheets, a significant increase in slab capacity becomes noticeable and slab toughness increases dramatically. It is obvious that the effect of CFRP started when slab reinforcement started yielding and first cracking load was not affected by these strengthened configurations, while yielding load increased somewhat, and the ultimate load and toughness of the strengthened slabs increased noticeably, and the slab exhibited a wide propagation of cracks.

Fig. 10 shows grouped load-deflection curves for flexural strengthened slabs S-5 to S-7, it is obvious that no significant change in ultimate load and in slab toughness in case of attaching 100 mm width CFRP sheet to full span of slab as S-5 or in case of attaching to 2/3S (1.40 m) as S-6. Attaching 100 mm width CFRP sheet to 1/3S (0.80 m) decreasing the slab capacity and toughness compared with attaching to 2/3S. Therefore, from the economical point of view, attaching 100 mm CFRP sheets to 2/3S optimizes the usage of CFRP sheets and gives same results if attached to full span of slab.

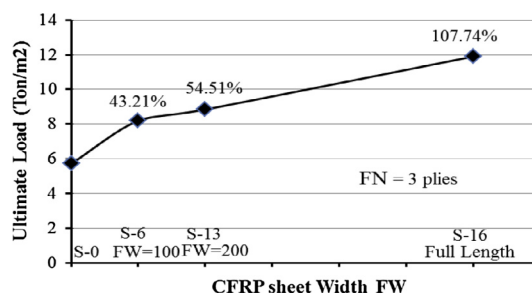
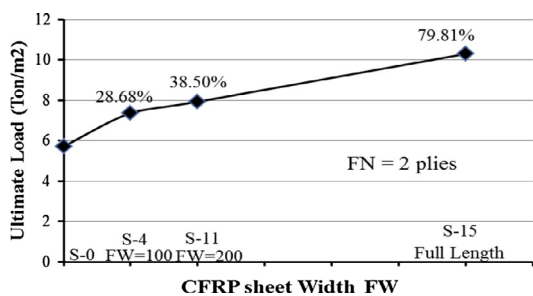


Figure 14 (a) UL versus FW at FN = 2 plies, and (b) UL versus FW at FN = 3 plies.

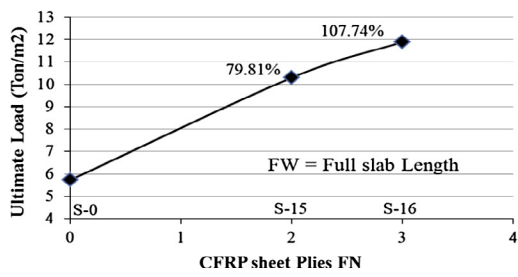
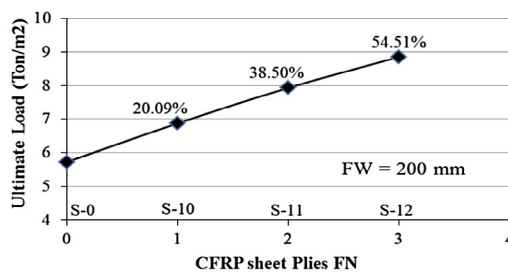
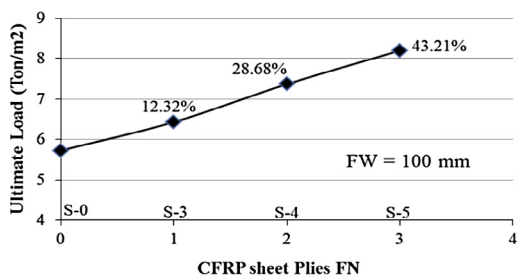


Figure 15 (a) UL versus FN at FW = 100 mm, (b) UL versus FN at FW = 200 mm, and (c) UL versus FN at FW = full slab length.

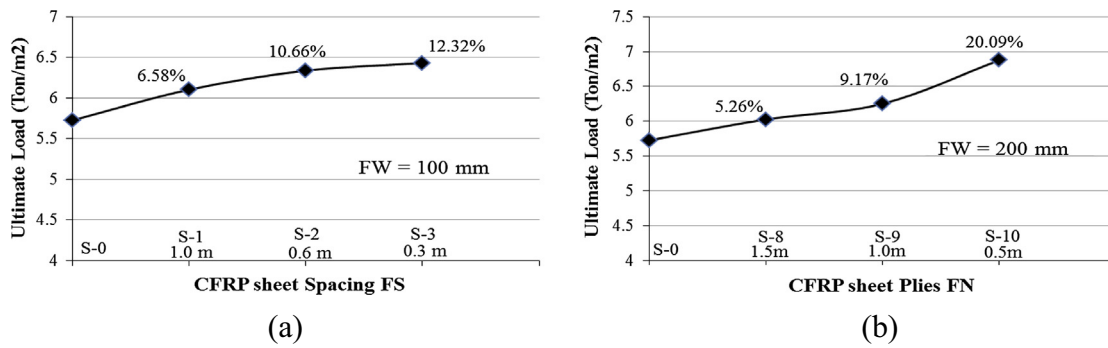


Figure 16 (a) UL versus FS at FW = 100 mm, and (b) UL versus FS at FW = 200 mm.

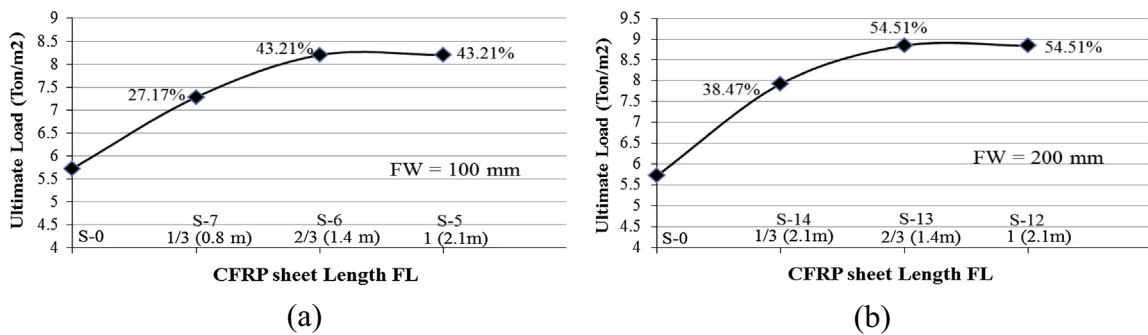


Figure 17 (a) UL versus FL at FW = 100 mm, and (b) UL versus FL at FW = 200 mm.

Fig. 11 shows grouped load–deflection curves for flexural strengthened slabs S-8 to S-14, it is obvious that by increasing the number of CFRP plies and decreasing the spacing between CFRP sheets, a significant increase in slab capacity becomes noticeable and slab toughness increases dramatically, and the slab exhibited a wide propagation of cracks.

Fig. 12 shows grouped load–deflection curves for flexural strengthened slabs S-12 to S-14, it is obvious that no significant change in ultimate load and in slab toughness in case of attaching 200 mm width sheets to full span of slab as S-12 or in case of attaching to 2/3S (1.40 m) as S-13. Attaching 200 mm width CFRP sheets to 1/3S (0.80 m) decreasing the slab capacity and toughness compared with attaching to 2/3S. Therefore, from the economical point of view attaching 200 mm CFRP sheets to 2/3S of optimizes the usage of CFRP sheet and gives same results if attached to full span of slab.

Fig. 13 shows grouped load–deflection curves for flexural strengthened slabs S-6, S-13, S-15, and S-16, it is obvious that by attaching the CFRP sheets to all slab length a significant increase in slab capacity becomes noticeable and slab toughness increases dramatically. Slab S15 shows increase in ultimate load by 80% and slab S16 shows increase in ultimate load by 108%, with obvious high strengthening ratios, but these two slabs exhibited a wide propagation of cracks until the failure.

5.4.2. Ultimate load UL versus CFRP sheet width FW

Fig. 14 shows the relationship between ultimate loads and CFRP sheet width FW; it is obvious that by increasing FW the ultimate load increases especially if CFRP sheet is attached to full slab length as in slab models S-15 and S-16.

5.4.3. Ultimate load UL versus CFRP sheet plies FN

Fig. 15 shows the relationship between ultimate load and CFRP sheet plies numbers FN, it is obvious that by increasing FN the ultimate load increases especially if the CFRP sheet is attached to a full slab length as in slabs S-15 and S-16.

5.4.4. Ultimate load UL versus CFRP sheet spacing FS

Fig. 16 shows the relationship between ultimate loads and CFRP sheet spacing FS, it is obvious that by decreasing FS the ultimate load increases.

5.4.5. Ultimate load versus CFRP sheet length FL

Fig. 17 shows the relationship between ultimate loads and CFRP sheet length FL, it is obvious that attaching CFRP sheet to slab span where FL = 1S (2.1 m) and 2/3S (1.4 m) gives the same ultimate load, while attaching CFRP sheet to 1/3S (0.8 m) reduces the ultimate load.

6. Conclusions

From the present study, it can be noticed that strengthening RC structures and bridges using Fiber-Reinforced Polymer (FRP) techniques allows preserving and keeping these buildings under nowadays standards. Moreover, this strengthening resists the increase in load levels in order to serve the new national development strategies, decreases financial funds for retrofitting processes, and the required time for retrofitting.

The previous study shows that strengthening of reinforced concrete slab (bridge deck) using CFRP sheets increases slab mechanical properties like strength, ductility, toughness, cracking behavior, and failure mode.

The following conclusions can be drawn based on the limited research reported in this paper.

- Three plies sheets with $FW = 100$ mm and $FW = 200$ mm schemes give result in a high development since they give increase in ultimate load between 43.2% and 54.8%, and the slab toughness will increase dramatically.
- Increasing CFRP sheet width (FW) increases the slab capacity and toughness.
- Using CFRP sheets attaching to the slab length give result in a very high development depending on the number of attaching plies, since they increase the ultimate load between 79.8% and 107.7%, the slab toughness will increase dramatically, and will exhibit a wide propagation of cracks until the failure.
- Attaching CFRP sheets to $2/3$ S gives same results of attaching to full slab span.
- Attaching CFRP sheets to $1/3$ S decreases the capacity of strengthening compared to attaching to slab span or $2/3$ S.
- Decreasing CFRP sheet spacing (FS) increases the slab capacity and toughness.

References

- [1] M. Arduini, A.D. Tommaso, A. Nanni, Brittle failure in FRP plate and sheet bonded beams, *ACI Struct. J.* (1997), July–August.
- [2] M. Arduini, A. Nanni, M. Ramgnolo, Performance of one way reinforced concrete slabs with externally bonded fiber reinforced polymer strengthening, *ACI Struct. J.* (2004), March–April.
- [3] U. Ebead, H. Marzouk, Fiber-reinforced polymer strengthening of two-way slabs, *ACI Struct. J.* (2004), September–October.
- [4] T.G. Ghoniem, Behavior of Concrete Masonry under axial Compression, Thesis no. 1058, AUC Library, Cairo, Egypt, 1990.
- [5] D. Kachlakev, T. Miller, S. Yim, K. Chansawat, T. Potisuk, Finite Element Modeling of Reinforced Concrete Structures Strengthening with FRP Laminates, Special Report SP316, Oregon Department Of Transportation, USA, May 2001.
- [6] Nabil F. Grace, George Abdel-Sayed, Wael F. Ragheb, Strengthening of concrete beams using innovative ductile fiber-reinforced polymer fabric, *ACI Struct. J.* (2002), September–October.
- [7] Regan M. Bramblett, Sergio F. Brena, Sharon L. Wood, Michael E. Kreger, Increasing flexural capacity of reinforced concrete beams using carbon fiber-reinforced polymer composites, *ACI Struct. J.* (2003), January–February.
- [8] Sergio F. Brena, Sharon L. Wood, Michael E. Kreger, Full-scale tests of bridge components strengthened using carbon fiber-reinforced polymer composites, *ACI Struct. J.* (2003), November–December.
- [9] A. Vasquez, V.M. Karbhari, Fiber reinforced polymer composite strengthening of concrete slabs with cutouts, *ACI Struct. J.* (2003), September–October.